

An Enclosed Paper Microfluidic Chip as a Sample Preconcentrator Based on Ion Concentration Polarization

Ning Liu , Dinh-Tuan Phan, and Wen Siang Lew, *Senior Member, IEEE*

Abstract—Sensitivity is an essential consideration for microfluidic paper-based analytical devices (μ PADs) when these devices are used for low concentration sample detection. Very recently, ion concentration polarization (ICP)-based μ PADs are emerging as novel tools for bio-sample preconcentration. In this study, we develop an enclosed paper-based microfluidic platform as a preconcentrator based on the ICP effect. This paper chip is fabricated by a Parafilm embedding technique and holds many advantages over traditional open-channel μ PADs, which usually suffer from sample contamination and evaporation problems. The enclosed structure minimizes sample evaporation, reduces contamination risk, and increases the mechanical strength of the paper channel. The experiment results show that more than 100-fold concentration enhancement can be achieved in the enclosed paper device, which is comparable with most reported paper-based ICP devices. Additionally, other improved ICP performance has been observed on the enclosed device, including better concentration plug profile, increased concentration durability.

Index Terms—Fabrication, ion concentration polarization, Lab-on-a-chip, paper-based microfluidics, Parafilm.

I. INTRODUCTION

THE development of inexpensive and practical assays with the capability of sensitively detecting diseases at the point-of-care (POC) is of great significance for global health [1], [2]. In recent years, numerous microfluidic devices have been developed as promising platforms for POC testing, biochemistry applications and fundamental research. For example, Guo demonstrated a novel prototype of smartphone based biosensor for clinical use [3]. Using various microfluidic device, Cairone *et al.* systematically studied the slug flow patterns generation,

a fundamental phenomenon in two-phase flow [4]. Microfluidic paper-based analytical devices (μ PADs), first proposed by Whitesides and colleagues [5] have received growing attention due to their excellent features, such as affordable, disposable and ease of fabrication. These paper-based assays are excellent candidate techniques for POC diagnostics [6], [7]. Despite these, there are still a lot of room to improve the performance of the existing μ PADs. Due to the traditional fabrication characteristics, most of the channels of μ PADs are exposed to the atmosphere. This open structure results in some drawbacks: 1) the sample in the open channel are easy to be contaminated; 2) the μ PADs suffer great liquid loss due to evaporation; 3) in some operations, the paper devices must be suspended in air to avoid contacting with any other solid surfaces to reduce contamination risk, however, this would increase the operation complications [8].

To address these issues, sealing techniques are required to enclose and protect the paper devices and several packing strategies have been proposed so far [9]. For example, Martinez *et al.* [8] introduced a fully enclosed μ PAD which was sealed by hydrophobic toner. They printed toner on both sides of a μ PAD using a color laser printer to create hydrophobic layers, which could effectively protect the reagents stored on the paper chip. They also used toner as adhesive layer and stack two single-ply channels on top of each other to construct an enclosed configuration, which can improve liquid sample delivery speed [10]. Fenton *et al.* [11] presented a method for paper-based lateral-flow test strips fabrication. They sandwiched porous nitrocellulose materials between vinyl cover tape and polyester plastic films to construct test strips. The packed device held the ability of reducing evaporation and protecting reagents from contamination. Fan *et al.* [12] developed laminated paper-based analytical devices (LPAD) by sandwiching paper strips between two polyester films. The bottom film was used to protect the strips and provide mechanical backing, and the sample could be loaded from the window located at the top film. To prepare the paper strip, they fixed chromatography paper to an adhesive carrier sheet and cut the paper using a cutting plotter. Renault *et al.* [13] described a method to fabricate hemichannels and fully enclosed channels. They printed wax pattern first on the top side of filter paper, and then turned over the printed paper and manually fed into the printer for printing on its bottom side. An interesting method that using triboelectric charges to

Manuscript received May 14, 2017; revised July 8, 2017; accepted July 9, 2017. Date of publication August 4, 2017; date of current version December 29, 2017. This work was supported in part by the Singapore National Research Foundation, Prime Minister's Office, under a Competitive Research Programme (Non-volatile Magnetic Logic and Memory Integrated Circuit Devices, NRF-CRP9-2011-01), in part by an Industry-IHL Partnership Program (NRF2015-IIP001-001), and in part by an RIE2020 AME-Programmatic Grant A1687b0033. This paper was recommended by Associate Editor Wendell Coltro. (*Corresponding author: Wen Siang Lew.*)

N. Liu and W. S. Lew are with the School of Physical and Mathematical Sciences, Nanyang Technological University, 637371, Singapore (e-mail: liun0006@e.ntu.edu.sg; wslew@pmail.ntu.edu.sg).

D.-T. Phan is with the Department of Biomedical Engineering, National University of Singapore, 117574, Singapore (e-mail: biepd@nus.edu.sg).

Color versions of one or more of the figures in this paper are available online at <http://ieeexplore.ieee.org>.

Digital Object Identifier 10.1109/TBCAS.2017.2727064

seal and control the flow in paper-based analytical devices was introduced by Silva *et al.* [14]. They used poly(ethylene terephthalate) (PET) film to seal a paper channel and rubbed the PET surface against acrylic or Teflon surfaces to generate triboelectric charges, leading to fluid delivery delay and evaporation decrease. However, the triboelectric charges cannot maintain for very long time. Hence, the device can minimize fluid evaporation only within short period.

Although advantageous, these reported sealing strategies have some drawbacks of their own. The adhesion of tape to paper substrate will severely deteriorate when the channels are wet. The printed toner provides good sealing effect but is not able to provide mechanical support for the paper channels. Many sealing methods are based on wax printing, however, spreading of the wax is difficult to control during heating, and incomplete melting of wax could lead to sample leakage. In addition, some sealing methods involve laborious fabrication or operation process.

Another challenge in μ PADs applications is to improve their sensitivity. Since that detection sensitivity is critical for POC applications, numerous approaches have been developed to tackle this challenge, such as field-amplified sample stacking (FASS) [15], [16], isotachopheresis (ITP) [17], [18], and temperature gradient focusing [19], [20]. Very recently, ion concentration polarization (ICP) technique has been introduced onto μ PADs as a sample pre-concentration approach with the aim to increase detection sensitivity [21], [22] or to integrate with a droplet microfluidic platform for bioassay [23], [24]. ICP is a fundamental electrokinetic effect that occurs at the interface of ion-selective nanostructures (i.e., nanochannels, Nafion junction formed by resin, or off-the-shelf membrane [25]) under the function of external electric field [26]. Based on ICP technique, Gong *et al.* [27] presented direct DNA analysis on paper-based microfluidic devices, where they concentrated and detected DNA samples on paper-based ICP devices and achieved comparable performance to the standard clinical equipment. Yeh *et al.* [28] improved ICP concentration performance by reducing paper channel depth, which resulted in decreased electroosmotic flow (EOF) speed. Phan *et al.* [29] demonstrated a 60-fold ICP pre-concentration enhancement on a paper microfluidic device cut by electric craft cutter. To maintain a steady fluid flow, Han *et al.* [30] integrated an absorbent pad on their paper ICP device and achieved up to 1000-fold pre-concentration factor.

To get over the drawbacks of open channel whilst enhancing the detection sensitivity of μ PADs, herein, we present an enclosed paper-based ICP pre-concentrator which is fabricated using a novel sealing method. The rapid-prototype of the μ PADs on the paper substrates can be achieved by electric craft cutting. The paper device is embedded by Parafilm from top and bottom side through simple heating and pressing process. Comparing with the existing sealing strategies mentioned above, our method possesses some unique features: 1) the pattern cut on parafilm-paper composite can be easily peeled off from adhesive cutting mat, reducing the likelihood of tears and rupture; 2) instead of wax, the using of Parafilm as sealing material can greatly reduce risk of sample leakage; 3) the Parafilm-paper composite displays much higher mechanical strength than wax printed devices.

II. EXPERIMENTAL SECTION

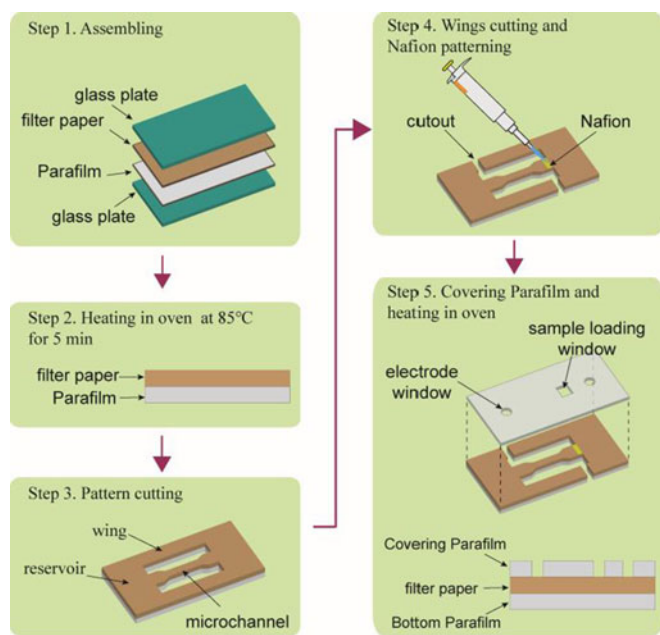
A. Materials and Experiment Setup

Sartorius quantitative grade 292 filter paper with average thickness of 180 μ m was used in the fabrication of laminar composite with Parafilm. Negatively charged fluorescein isothiocyanate (FITC) (Sigma-Aldrich) solution with concentration of 5 μ M was used as fluorescent tracer during the ICP process. Nafion perfluorinated ion exchange resin (Sigma-Aldrich) was directly patterned on paper channel to form a permselective membrane.

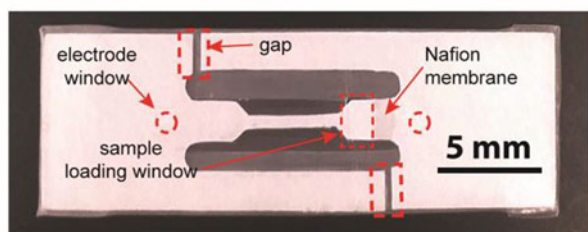
An inverted fluorescence microscope (Nikon Eclipse Ti-S) equipped with a CCD camera (Nikon DS-Ri2) was used to capture all images in the experiment. A customized Python program was developed to quantitatively analyze the captured images. A power supply (PLH250-P, Aim and Thurlby Thandar Instruments, UK) was used to provide the external electrical field to induce ICP on the paper chip. The standard tensile strength test was carried out on different substrates using a mechanical testing machine (YG026B electronic fabric strength tester).

B. Device Fabrication and Operation

The procedures of fabricating the enclosed μ PADs were illustrated in Fig. 1(a), including five major steps. First, the Parafilm and filter paper were laminated and sandwiched between two glass plates using clamps. Next, the parafilm laminated with filter paper was placed in oven at 85 $^{\circ}$ C for 5 minutes. Due to the wax property of paraffin, the Parafilm gradually melted and partially penetrated into the porous filter paper, forming a two-layer composite. The melted Parafilm bonded the filter paper very tightly and formed a Parafilm-paper composite. In the third step, the obtained Parafilm-paper composite was sent to cut using a computer controlled craft cutter (Silhouette America, Inc., Silhouette Cameo) to obtain the designed microchannel. Meanwhile, the covering Parafilm bearing sample loading window and electrode windows was also prepared using the craft cutter. In step 4, the two wings of the device were cut manually to leave the microchannel as the only path connecting two reservoirs. Therefore, each wing of the device worked as the extension of one reservoir to absorb more water, enhancing moisture retention capability of the device. On the paper device, 0.5 μ L Nafion perfluorinated resin was directly pipetted at one end of the microchannel and left at room temperature about 1 h for air-drying. In the last step, the covering Parafilm and Parafilm-paper substrate was aligned and placed in oven for 3 minutes at 85 $^{\circ}$ C to enable the covering layer to tightly bond with the filter paper from top side. To reduce liquid sample leakage, the dimension of the covering Parafilm was slightly larger than that of the Parafilm-paper substrate. The extra margin of covering Parafilm was folded back to wrap the edges of the reservoirs. Finally, an enclosed paper-based device was fabricated with the paper microchannel was sandwiched by two Parafilm from top and bottom side. The electrode windows on the covering Parafilm can allow the electrodes to directly touch the hydrophilic paper reservoirs. Due to the small dimension of the window, the amount of evaporation loss from the window was very little.



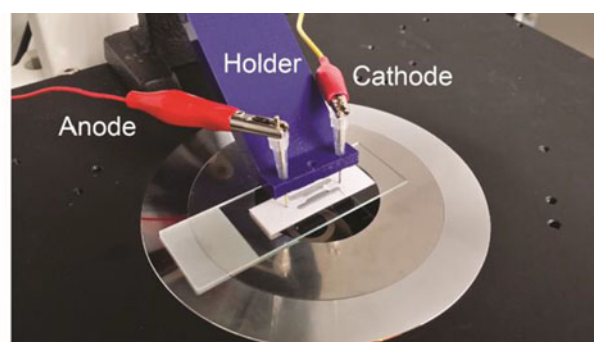
(a)



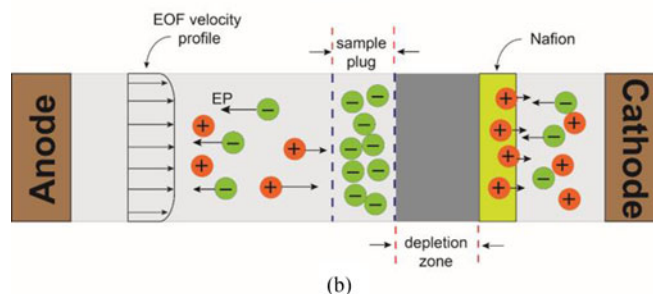
(b)

Fig. 1. (a) Schematic illustration of the device fabrication process. (b) The photograph of an enclosed paper-based pre-concentrator. Two gaps were cut on the two wings, leaving the microchannel as the only path connecting the two reservoirs. Two electrode windows were located in the two reservoirs, respectively.

As shown in Fig. 2(a), two copper electrodes were mounted on a 3D printed holder and placed on the paper device to provide electric voltage. To operate the device, the channel and reservoirs were firstly pre-wetted with 10 mM CaCl_2 solution, followed by loading $5 \mu\text{L}$ sample from the sample loading window. Fluorescence images were captured every 10 s for subsequent analysis. The basic working principle of ICP pre-concentration was demonstrated in Fig. 2(b). The Nafion membrane is composed of nanopores with average diameter of 4 nm. The surfaces of the pores are negatively charged due to the existence of sulfonic acid groups in Nafion, resulting in only cations can transport through the Nafion membrane. Under external voltage, the cations move toward the cathode and can transport through the Nafion membrane. On the contrary, anions at the right side of Nafion cannot travel through the membrane. To satisfy electrical neutrality, the continuous efflux of cations at the anodic side of membrane results in anions moving out of this region. The electrophoretic migration (EP) is dominant in the depletion region and pushes the negatively charged FITC ions toward the anodic side. While the electroosmotic flow (EOF), which is dominant downstream of the depletion region, drives the fluorescent tracers to move



(a)



(b)

Fig. 2. (a) Close view of the μPAD with two electrodes fixed by a 3D printed holder. (b) Schematic illustration of ICP induced by external electric field. The Nafion permselective film only allow cations to pass through. Ion depletion region forms at the anodic side of Nafion, repelling negatively charged analytes toward the anode.

toward the cathodic side [27]. The balance of the two opposing effects leads to the tracers focused at the depletion boundary.

III. RESULTS AND DISCUSSION

A. Parafilm Sealing Method

Parafilm, a thermoplastic material consisting primarily of polyolefins and paraffin waxes, is widely used in biology and chemistry laboratories, and recently has found its special use to fabricate paper-based microfluidic devices [31], [32]. Distinct from the previous reports where the Parafilm were used to form hydrophobic barriers to define the microchannel, in our μPAD , the Parafilm offers a leakproof surface to enclose the paper microchannel. The cross-sectional views of Parafilm-paper composites were captured by optical microscope and showed in Fig. 3. Before heating, the boundary between filter paper and Parafilm can be clearly seen in Fig. 3(a). Fig. 3(b) showed a filter paper embedded from bottom side. During heating process (85°C , 5 minutes), the Parafilm melted and became semi-liquid, which gradually penetrated into the microporous paper under the pressure from clamped glass plates, resulting in that the Parafilm and filter paper bond tightly. The fibres were submerged by semi-liquid paraffin wax, forming a condensed composite that was difficult to be peeled off even when the paper is wet. This is advantageous over many other sealing methods that cannot withstand wet situation. The original thicknesses of Parafilm and filter paper were $130 \mu\text{m}$ and $180 \mu\text{m}$ respectively. The Parafilm embedding process led to the total thickness decreased to less

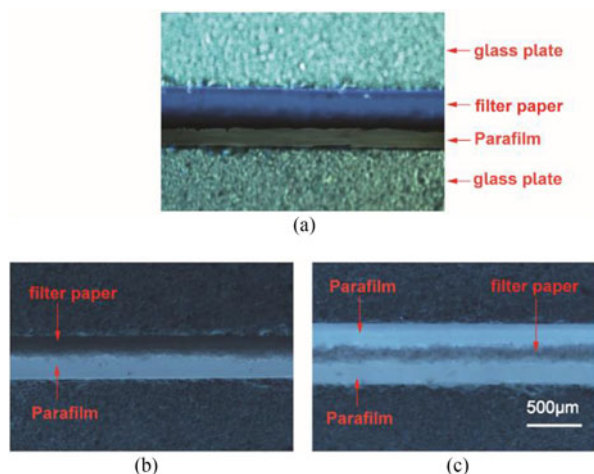


Fig. 3. Cross sectional view of the Parafilm and paper. (a) a filter paper and parafilm laminated together before heating; (b) a filter paper penetrated by Parafilm from bottom side; (c) a filter sandwiched by two layers Parafilm after heating.

than $280\ \mu\text{m}$, indicating that the Parafilm has been pressed into the paper. Fig. 3(c) indicated that a filter paper was embedded by two Parafilm layers from top and bottom side. The filter paper remained hydrophilic and worked as an enclosed channel. The Parafilm penetration depth depends on heating time, temperature and applied pressure to press the melted Parafilm into porous paper. Through adjusting the three factors, the hydrophilic channel thickness can be well controlled. Additionally, as a mechanical process, craft cutting can guarantee reproduction accuracy and high consistency from sample to sample. Therefore, the fabrication method is highly reproducible and has the potential for mass production of μPADs .

Electric craft cutting provides an ideal choice for rapid-prototype of paper-based devices. However, some researchers reported that the tearing and rupture occurred very often when craft cutter was used for cutting cellulose filter paper [11], [33], [34]. In addition, to fix the paper before implementing craft cutting, the paper substrates must be stick to adhesive surface of a cutting mat. However, when they are peeled off from the adhesive mat, small structures are easily broken due to their low mechanical strength. In our fabrication process, we compared the cutting performance on the Parafilm-paper composite and bare filter paper. As shown in Fig. 4(a) and (b), in contrary to using bare paper [see Fig. 4(a)], the use of Parafilm-paper laminar composite [see Fig. 4(b)] allowed the cutting process to be performed smoothly without any tears. This can be attributed to two factors: first, the surface of Parafilm was much smoother than that of bare filter paper; second, the laminar composite was much more robust than bare filter paper. Additionally, thanks to enhanced mechanical strength, the small structures cut on this composite can be easily peeled off from adhesive mat without broken.

B. Mechanical Property Test

Low mechanical strength is a major weakness of most existing paper-based microfluidic devices. Particularly, the paper

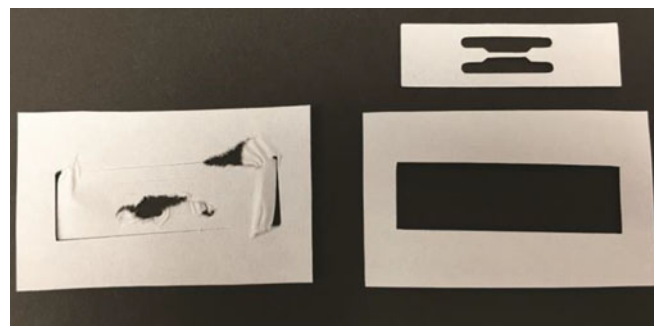


Fig. 4. Comparison of cutting performances on (a) bare filter paper and (b) Parafilm-paper composite. Tears and ruptures occurs very often when filter paper was used as substrate for craft cutting, this can be attributed to the rougher texture of filter paper comparing with printing paper. For the Parafilm-paper composite, since one side was covered with smooth Parafilm, the cutting can be performed smoothly without tears and ruptures.

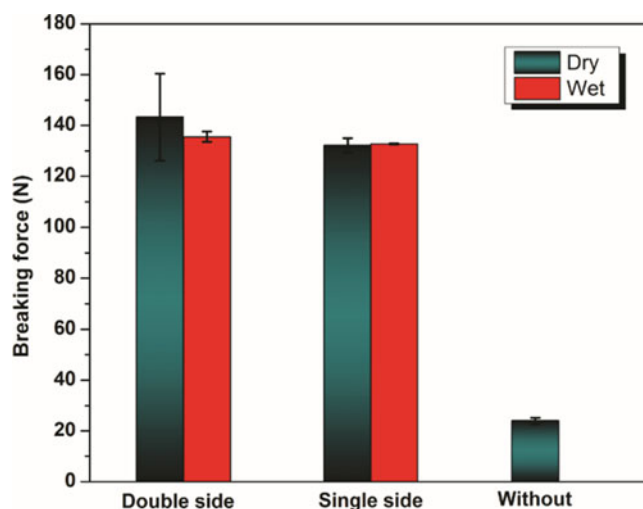


Fig. 5. Mechanical strength test of different paper substrates. Due to the super-low mechanical strength of wet filter paper, the test was only performed on bare filter paper in dry state. Each force value is averaged over $N = 4$ measurements. The error bars represent one standard deviation.

channels cut by knife possess relative low strength due to reduced physical dimension. The problem is even more severe when the paper channel is wetted by aqueous samples. In many circumstances, the paper channel becomes sagging when liquid samples are loaded onto the channel. This is because that the mechanical strength of cellulose fibres dramatically decreases when the fibres are wetted. Therefore, to prevent the wet channel from contacting surrounding solid surfaces (e.g., glass plate on microscope stage), the paper devices with open channels usually must be suspended in air, which may cause the operation to be complicated. As mentioned above, the Parafilm-paper laminar composite showed high mechanical strength, which facilitated the uniform appearance and the large-scale fabrication of μPADs .

To demonstrate how well the mechanical strength had been enhanced by Parafilm embedding, a standard tensile stress-strain test was carried out on different paper substrates. Fig. 5 depicted the forces required to pull different substrates to the points where

they broke. The paper substrates with double side embedded by Parafilm and single side embedded by Parafilm were tested in dry state and wet state. The bare filter paper without Parafilm embedding was only tested in dry state, due to that wet filter paper possessed super low mechanical strength that below the minimum range of the strength tester. In dry state, the filter paper had the highest breaking force of 25.8 N. While in dry state, the double side embedded and single side embedded substrates showed highest breaking forces of 160 N and 134 N, respectively. Even in wet state, these two Parafilm embedded substrates remained high mechanical strength. For the paper sealed from double side, the standard deviation regarding the breaking force is much higher than that of single side embedded substrates. This should be attributed to lamination nonuniformity used for fabricating double side embedded paper. When the double side embedded paper underwent tensile strength test, usually only one side Parafilm broke first. Hence, the test results of the double side embedded are similar as those of single side embedded device. The results proved that the Parafilm embedding technique dramatically enhanced the mechanical property of paper substrates.

C. ICP Demonstration on Enclosed μ PADs

At the beginning of the experiment, a drop of 20 μ M fluorescent tracer in deionized water was dipped onto the sample loading window of the paper channel. The entire channel was pre-wetted in 2 ~ 3 minutes due to the capillary effect of the cellulose paper. A voltage was applied across the channel through two copper electrodes connected with power supply to trigger ICP.

Experimental results for ion depletion and concentration were shown in Fig. 6. Fluorescence images were recorded at different time (150 s, 200 s, 250 s, 300 s, 450 s) with a constant voltage of 50 V. Here, the time when the power supply started to provide voltage was set as start time point. The time-lapse images in Fig. 6(a) demonstrated the ion depletion at the anodic side of the Nafion membrane developed and expanded with time under a DC voltage. The generation of ICP was based on the permselectivity (cation-biased conductance) of Nafion membrane. Due to the existence of sulfonic acid groups in Nafion membrane, the surfaces of the nanopores were negatively charged, resulting in the selective migration of cations while the anions were blocked at the boundary of the membrane. The cations continuously migrated to the cathode under the function of external electric field. The fluorescent tracer used here was negatively charged and repelled by the ion depletion region toward anode. Consequently, the ion depletion region was induced at the interface of paper channel and nanoporous membrane. Previous studies demonstrated that the geometry of the paper channel can influence the concentration effect. Usually, a convergent channel can generate high pre-concentration effect than a straight channel [35], [36]. Gong *et al.* [35] used this arrangement to enhance sample pre-concentration and Yang *et al.* [36] systematically investigated the effect for paper-based ICP. In our study, we adopted convergent channel design to improve the device performance. The sample loading zone interfaced with the straight channel

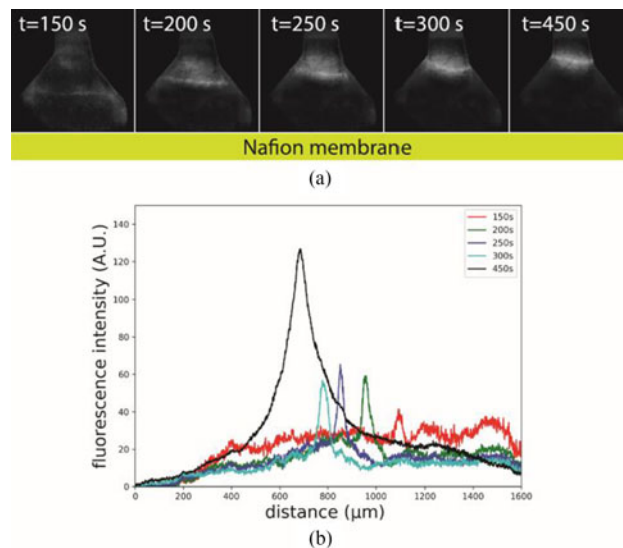


Fig. 6. Formation of depletion region and concentration plug in sample loading region of an enclosed μ PAD. The sample loading region has a nozzle-like shape to produce a better concentration effect. (a) Time sequential images of 5 μ M FITC in the sample loading region under an applied voltage of 50 V. The time when the power supply started to provide voltage was set as start time point. (b) The corresponding fluorescence intensity profiles at selected time points are plotted. The maximum concentration of FITC fluorescent dye reaches more than 100-fold at 250 s.

with a convergent geometry. The variation of channel dimension caused a nozzle-like squeeze effect. The pre-concentration performance was greatly enhanced by the nozzle at 250 s, resulting in more than 100-fold pre-concentration [see Fig. 6(b)].

Fig. 7(a) demonstrates the pre-concentration plug moving in the enclosed straight channel. The boundary of depletion region became more and more bright, indicating the continuous accumulation of fluorescence ions. The forming of concentration band at the anodic side of depletion region boundary resulted from the balance of electroosmotic flow (EOF) and electrophoretic migration (EP). The EP was dominant in the depletion region, forcing the negatively charged fluorescent ions migrate toward the anodic direction. While in the downstream of the depletion region, the EOF was dominant and drove the fluorescent tracers to the boundary of the depletion region. The interaction of the two opposing effects finally resulted in the concentration phenomenon. For observation convenience, we set the time when the concentration plug entered the straight channel as start time point. To quantitatively analyze the concentration effect, the corresponding fluorescence intensity profiles were shown in Fig. 7(b), where the concentration enhancement reached its maximum at 150 s. The calculated maximum pre-concentrator factor is 60-fold. It can also be observed from the images that the pre-concentration plug gradually dispersed after 450 s, indicating the decreased ICP effect. This decrease can be attributed to the accumulated sample evaporation loss through the sample loading window and electrode windows. The results clearly demonstrated that the sensitivity of the paper-based assay was substantially improved by ICP effect.

Moreover, the enclosed configuration also enhanced the ICP durability. The fluorescence profiles showed that the

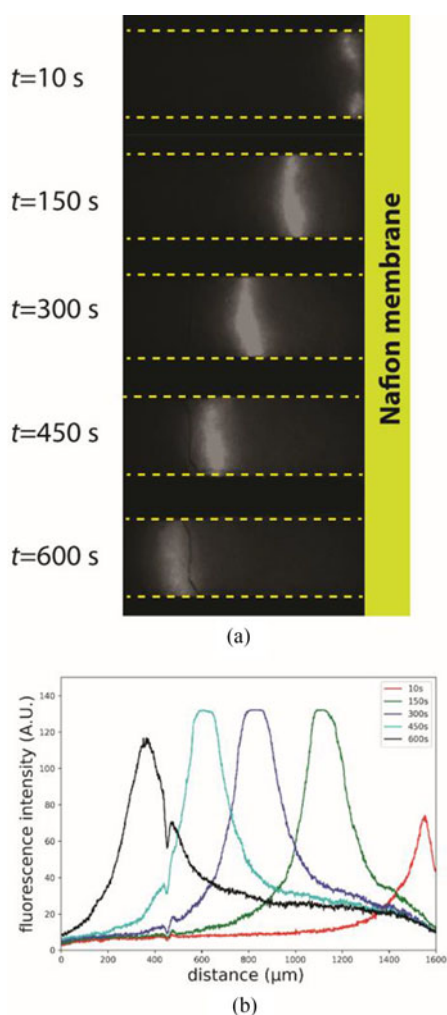


Fig. 7. Movement of pre-concentration plug in an enclosed straight channel downstream of the sample loading region. (a) time sequential images (b) and corresponding fluorescence intensity profiles of the pre-concentration plug are recorded at selected time points. The boundaries of the paper channels are indicated by the dashed lines. the concentration enhancement reached its maximum at 150 s and maintained at its maximum level for more than 300 s.

pre-concentration plug can maintain around its maximum level for more than 300 s. The enhanced durability proved that the enclosed ICP device is suitable for practically point-of-care detection. The images of Fig. 7(a) indicated that the profiles of the pre-concentration plug were more regular and concentrated than that we previously reported [29]. It has been reported that the fibre orientation plays an essential role on fluid flow in porous paper [37], [38]. However, in our fabrication process, the external pressure, which was applied from top and bottom side to press the melted Parafilm into the porous paper, could not change the fibre orientation in the paper. Therefore, we speculate that the porous paper was tightly compressed during Parafilm embedding process, resulting in regular alignment of the micropores.

In contrast to recently reported paper-based ICP pre-concentrator, most of which were fabricated by wax printing and directly exposed to air, the Parafilm embedded paper device can

effectively prevent direct sample contact with support substrate, resulting in reduced sample contamination possibility, as well as dramatically mitigated sample evaporation rate. In addition, the mechanical strength of open-channel ICP pre-concentrator is deteriorated in wet state, leading to numerous operation inconvenience. Contrarily, the high mechanical strength of our proposed μPAD can increase device operation flexibility.

Maintaining steady flow is of great significance to achieve high pre-concentration factor. Through adding external absorbent pad, Han *et al.* achieved up to 1000-fold pre-concentration result. The external absorbent pad maintained the paper channel in fully wet state. However, the addition of an external pad increased the operational complexity. Moreover, since the absorbent is exposed to atmosphere, the liquid evaporation loss is significant. Comparing to the recently reported ICP paper-based devices, which achieved up to several hundred-fold concentration factor [28], [30], [35], our device has its own advantages. Departing from the method using external absorbent pad, we fabricated two reservoirs with microchannel on single paper substrate. The reservoirs act as absorbent pads to keep the pressure difference, which is the driven source of the lateral flow in the paper channel, remained constant throughout the period of experiment. The sealing configuration not only increases the device portability but also facilitates operational simplicity.

D. Mitigated Evaporation Influence

Traditional μPADs with open channels are susceptible to evaporation. Liquid sample loss and concentration change caused by evaporation are common problems suffered by open paper fluidic channels. These issues are even more severe when dealing with precious samples. Specifically, in term of paper-based ICP, voltage induced Joule heating could deteriorate the situation. On paper-based ICP device, the ion migration is primarily affected by the conductance of the channel. Hence, the moisture retention is of significance to keep ICP effect on the paper device. One of the most important advantages of the enclosed μPAD is that it can dramatically mitigate sample evaporation. To demonstrate the capability of our device of mitigating evaporation, fluorescent tracer pre-concentration was performed on an enclosed paper-based ICP device. In this experiment, the pre-wetted paper device was placed in atmosphere at room temperature for 2 hours, followed by applying 50 V voltage to trigger ICP. The corresponding ICP effect was reflected by the images in Fig. 8(a). The time sequential images demonstrate that the sample was gradually concentrated and moved away from the Nafion membrane. This implies that an ICP effect was induced at the anodic side of the permselective membrane and can maintain for very long time without outside reagent supply. Even was left in atmosphere for 2 hours, an ICP phenomenon could still be induced on the enclosed device, indicating that the paper channel remained good conductance. This should be attributed to the protection of the Parafilm packing, which greatly reduced the evaporation rate of the liquid reagent in the device. Particularly, the two reservoirs sealed by Parafilm played an essential role in moisture retention. We previously reported 60-fold concentration enhancement on another paper-based ICP

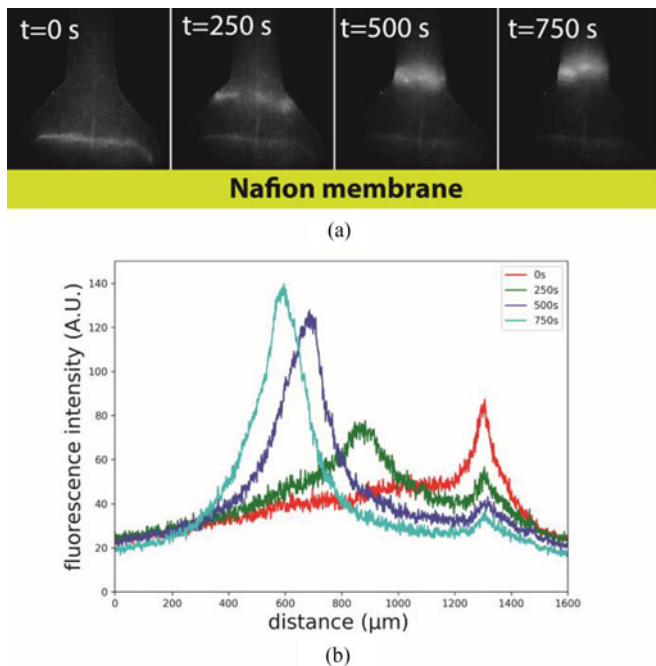


Fig. 8. ICP performance on the pre-wetted enclosed μ PAD that has been left in atmosphere for 2 hours: (a) time sequential images and (b) corresponding fluorescence intensities of pre-concentration plug at different time points. The time point of applying external voltage was set as $t = 0$.

pre-concentrator, which was cut by craft cutter and sealed using Scotch film to reduce sample evaporation [29]. However, sample leakage occurred in the device due to the deteriorated film adhesion when the channels were wet. In the contrary, the sample leakage is effectively prevented in the Parafilm enclosed device.

IV. CONCLUSION

In summary, we reported a novel and cost-effective enclosed paper microfluidic platform based on ICP as sample pre-concentrator. A Parafilm embedding technique was introduced to fabricate enclosed paper devices. This technique exploits easy-to-access materials and does not need expensive equipment. And the fabrication process is simple and easy-to-handle, enabling the possibility of large scale production of μ PADs. The strain-stress testing quantitatively proved that the Parafilm-paper composite held great mechanical strength. On the enclosed μ PAD, more than 100-fold pre-concentration factor has been achieved, demonstrating a good concentration performance that was comparable with many reported paper-based ICP devices. Comparing to traditional open channel μ PADs, the Parafilm embedded paper device as ICP platform possesses four major advantages: 1) the Parafilm encased chip shows stronger mechanical strength than a pure paper chip; 2) it shows better concentration profile than on open-channel device; 3) it greatly reduces sample contamination risk thanks to the enclosed configuration; 4) it holds the capability of dramatically mitigating nature evaporation during a relatively long period. We believe that our enclosed microfluidic devices are suitable for generic

biochemical assays and therefore pave an avenue to overcome some major problems of conventional open-channel devices.

ACKNOWLEDGMENT

The authors declare no financial or commercial conflicts of interest.

REFERENCES

- [1] A. J. Tudos, G. A. J. Besselink, and R. B. M. Schasfoort, "Trends in miniaturized total analysis systems for point-of-care testing in clinical chemistry," *Lab Chip*, vol. 1, pp. 83–95, 2001.
- [2] C. D. Chin, V. Linder, and S. K. Sia, "Lab-on-a-chip devices for global health: Past studies and future opportunities," *Lab Chip*, vol. 7, pp. 41–57, 2007.
- [3] J. H. Guo, "Uric acid monitoring with a smartphone as the electrochemical analyzer," *Anal. Chem.*, vol. 88, pp. 11986–11989, Dec. 2016.
- [4] F. Cairone, S. Gagliano, and M. Bucolo, "Experimental study on the slug flow in a serpentine microchannel," *Exp. Therm. Fluid Sci.*, vol. 76, pp. 34–44, Sep. 2016.
- [5] A. W. Martinez, S. T. Phillips, M. J. Butte, and G. M. Whitesides, "Patterned paper as a platform for inexpensive, low-volume, portable bioassays," *Angew. Chem. Int. Ed.*, vol. 46, pp. 1318–1320, 2007.
- [6] A. K. Yetisen, M. S. Akram, and C. R. Lowe, "Paper-based microfluidic point-of-care diagnostic devices," *Lab Chip*, vol. 13, pp. 2210–2251, Jun. 2013.
- [7] Y. Y. Xia, J. Si, and Z. Y. Li, "Fabrication techniques for microfluidic paper-based analytical devices and their applications for biological testing: A review," *Biosens. Bioelectron.*, vol. 77, pp. 774–789, Mar. 2016.
- [8] K. M. Schilling, A. L. Lepore, J. A. Kurian, and A. W. Martinez, "Fully enclosed microfluidic paper-based analytical devices," *Anal. Chem.*, vol. 84, pp. 1579–1585, Feb. 2012.
- [9] X. Jiang and Z. H. Fan, "Fabrication and operation of paper-based analytical devices," *Annu. Rev. Anal. Chem.*, vol. 9, pp. 203–222, 2016.
- [10] C. K. Camplisson, K. M. Schilling, W. L. Pedrotti, H. A. Stone, and A. W. Martinez, "Two-ply channels for faster wicking in paper-based microfluidic devices," *Lab Chip*, vol. 15, pp. 4461–4466, 2015.
- [11] E. M. Fenton, M. R. Mascarenas, G. P. Lopez, and S. S. Sibbett, "Multiplex lateral-flow test strips fabricated by two-dimensional shaping," *ACS Appl. Mater. Interfaces*, vol. 1, pp. 124–129, Jan. 2009.
- [12] C. L. Cassano and Z. H. Fan, "Laminated paper-based analytical devices (LPAD): Fabrication, characterization, and assays," *Microfluidics Nanofluidics*, vol. 15, pp. 173–181, Aug. 2013.
- [13] C. Renault, J. Koehne, A. J. Ricco, and R. M. Crooks, "Three-dimensional wax patterning of paper fluidic devices," *Langmuir*, vol. 30, pp. 7030–7036, Jun. 2014.
- [14] E. T. S. G. da Silva, M. Santhiago, F. R. de Souza, W. K. T. Coltro, and L. T. Kubota, "Triboelectric effect as a new strategy for sealing and controlling the flow in paper-based devices," *Lab Chip*, vol. 15, pp. 1651–1655, 2015.
- [15] B. Jung, R. Bharadwaj, and J. G. Santiago, "Thousandfold signal increase using field-amplified sample stacking for on-chip electrophoresis," *Electrophoresis*, vol. 24, pp. 3476–3483, Oct. 2003.
- [16] J. Lichtenberg, E. Verpoorte, and N. F. de Rooij, "Sample preconcentration by field amplification stacking for microchip-based capillary electrophoresis," *Electrophoresis*, vol. 22, pp. 258–271, Jan. 2001.
- [17] B. Jung, R. Bharadwaj, and J. G. Santiago, "On-chip millionfold sample stacking using transient isotachopheresis," *Anal. Chem.*, vol. 78, pp. 2319–2327, Apr. 2006.
- [18] S. S. Bahga, R. D. Chambers, and J. G. Santiago, "Coupled isotachopheretic preconcentration and electrophoretic separation using bidirectional isotachopheresis," *Anal. Chem.*, vol. 83, pp. 6154–6162, Aug. 2011.
- [19] T. Matsui, J. Franzke, A. Manz, and D. Janasek, "Temperature gradient focusing in a PDMS/glass hybrid microfluidic chip," *Electrophoresis*, vol. 28, pp. 4606–4611, Dec. 2007.
- [20] D. Ross and L. E. Locascio, "Microfluidic temperature gradient focusing," *Anal. Chem.*, vol. 74, pp. 2556–2564, Jun. 2002.
- [21] Y. C. Wang, A. L. Stevens, and J. Y. Han, "Million-fold preconcentration of proteins and peptides by nanofluidic filter," *Anal. Chem.*, vol. 77, pp. 4293–4299, Jul. 2005.

- [22] J. H. Lee, Y. A. Song, and J. Y. Han, "Multiplexed proteomic sample preconcentration device using surface-patterned ion-selective membrane," *Lab Chip*, vol. 8, pp. 596–601, 2008.
- [23] C. H. Chen *et al.*, "Enhancing protease activity assay in droplet-based microfluidics using a biomolecule concentrator," *J. Amer. Chem. Soc.*, vol. 133, pp. 10368–10371, Jul. 2011.
- [24] D. T. Phan, Y. Chun, and N. T. Nguyen, "A continuous-flow droplet-based concentrator using ion concentration polarization," *RSC Adv.*, vol. 5, pp. 44336–44341, 2015.
- [25] D. T. Phan, C. Yang, and N. T. Nguyen, "Fabrication of nanoporous junctions using off-the-shelf Nafion membrane," *J. Micromech. Microeng.*, vol. 25, Nov. 2015, Art. no. 115019.
- [26] S. J. Kim, Y. A. Song, and J. Han, "Nanofluidic concentration devices for biomolecules utilizing ion concentration polarization: Theory, fabrication, and applications," *Chem. Soc. Rev.*, vol. 39, pp. 912–922, 2010.
- [27] M. M. Gong, R. Nosrati, M. C. S. Gabriel, A. Zini, and D. Sinton, "Direct DNA analysis with paper-based ion concentration polarization," *J. Amer. Chem. Soc.*, vol. 137, pp. 13913–13919, Nov. 2015.
- [28] S. H. Yeh, K. H. Chou, and R. J. Yang, "Sample pre-concentration with high enrichment factors at a fixed location in paper-based microfluidic devices," *Lab Chip*, vol. 16, pp. 925–931, 2016.
- [29] D. T. Phan, S. A. M. Shaegh, C. Yang, and N. T. Nguyen, "Sample concentration in a microfluidic paper-based analytical device using ion concentration polarization," *Sens. Actuators B-Chem.*, vol. 222, pp. 735–740, Jan. 2016.
- [30] S. I. Han, K. S. Hwang, R. Kwak, and J. H. Lee, "Microfluidic paper-based biomolecule preconcentrator based on ion concentration polarization," *Lab Chip*, vol. 16, pp. 2219–2227, 2016.
- [31] E. M. Dunfield, Y. Wu, M. T. Koesdjojo, T. P. Remcho, and V. T. Remcho, "Simple and rapid fabrication of paper microfluidic devices utilizing Parafilm," 2012. [Online]. Available: <http://blogs.rsc.org/chipsandtips/2012/04/10/simple-and-rapid-fabrication-of-paper-microfluidic-devices-utilizing-parafilm>
- [32] L. Yu and Z. Z. Shi, "Microfluidic paper-based analytical devices fabricated by low-cost photolithography and embossing of Parafilm (R)," *Lab Chip*, vol. 15, pp. 1642–1645, 2015.
- [33] X. E. Fang, S. S. Wei, and J. L. Kong, "Paper-based microfluidics with high resolution, cut on a glass fiber membrane for bioassays," *Lab Chip*, vol. 14, pp. 911–915, 2014.
- [34] R. A. G. de Oliveira, F. Camargo, N. C. Pesquero, and R. C. Faria, "A simple method to produce 2D and 3D microfluidic paper-based analytical devices for clinical analysis," *Anal. Chim. Acta*, vol. 957, pp. 40–46, Mar. 2017.
- [35] M. M. Gong, P. Zhang, B. D. MacDonald, and D. Sinton, "Nanoporous membranes enable concentration and transport in fully wet paper-based assays," *Anal. Chem.*, vol. 86, pp. 8090–8097, Aug. 2014.
- [36] R. J. Yang, H. H. Pu, and H. L. Wang, "Ion concentration polarization on paper-based microfluidic devices and its application to preconcentrate dilute sample solutions," *Biomicrofluidics*, vol. 9, Jan. 2015, Art. no. 014122.
- [37] K. Tenda, R. Ota, K. Yamada, T. G. Henares, K. Suzuki, and D. Citterio, "High-resolution microfluidic paper-based analytical devices for sub-microliter sample analysis," *Micromachines*, vol. 7, May 2016, Art. no. 80.
- [38] Y. Xu and T. Enomae, "Paper substrate modification for rapid capillary flow in microfluidic paper-based analytical devices," *RSC Adv.*, vol. 4, pp. 12867–12872, 2014.

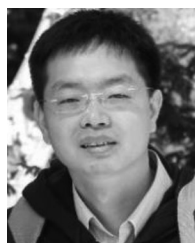


Ning Liu received the B.S. degree from the North University of China, Taiyuan, China, and the M.Eng. degree from Beijing University of Technology, Beijing, China, in 2009 and 2012, respectively. Currently, he is working toward the Ph.D. degree at the Nanyang Technological University, Singapore.

His research interests include cell separation and manipulation in microfluidic devices, microfabrication, and paper-based microfluidics.



Dinh-Tuan Phan received the Ph.D. degree from the Nanyang Technological University, Singapore, in 2016 under the supervisions of Prof. Nam-Trung Nguyen and Prof. Charles Chun Yang. Currently, he is a Postdoctoral Research Fellow with the National University of Singapore. He is doing research on the fabrication of nanofluidic devices and nanofluidic phenomena, especially ion concentration polarization and its bio-applications.



Wen Siang Lew (SM'13) received the Ph.D. degree from the University of Cambridge, Cambridge, U.K., in 2002. He is an Associate Professor with the Nanyang Technological University, Singapore. His research interests include spintronics devices, nanomagnetism, bioMEMS devices, and emerging nanomaterials. He is a member of the Singapore Spintronics Consortium.